Singular behavior of the spectrum in the neighborhood of focus

Greg Gbur

Department of Physics and Astronomy and The Institute of Optics, University of Rochester, River Campus Station, Rochester, New York 14627-0171

Taco D. Visser

Department of Physics and Astronomy, Free University, De Boelelaan 1081, 1081 HV Amsterdam, The Netherlands, and Department of Physics and Astronomy, University of Rochester, River Campus Station, Rochester, New York 14627-0171

Emil Wolf

Department of Physics and Astronomy and The Institute of Optics, University of Rochester, River Campus Station, Rochester, New York 14627-0171

Received January 18, 2002; accepted March 12, 2002

In a recent paper [Phys. Rev. Lett. **88**, 013901 (2002)] it was shown that when a convergent spatially coherent polychromatic wave is diffracted at an aperture, remarkable spectral changes take place on axis in the neighborhood of certain points near the geometrical focus. In particular, it was shown that the spectrum is redshifted at some points, blueshifted at others, and split into two lines elsewhere. In the present paper we extend the analysis and show that similar changes take place in the focal plane, in the neighborhood of the dark rings of the Airy pattern.

OCIS codes: 260.1960, 030.1670, 300.6170.

1. INTRODUCTION

At points of wave fields where the intensity has zero value, the phase becomes undetermined and the structure of the field in the neighborhood of such points has a rather complicated structure. It may exhibit, for example, optical vortices or wave-front dislocations. The study of such structures has developed into a new discipline, sometimes called *singular optics*.[1,2] Investigations on this topic have been almost exclusively confined to monochromatic wave fields. (Notable exceptions are Refs. 3 and 4, which deal with the colors of caustics).

In a recent paper[5] we showed that in some polychromatic wave fields another unusual phenomenon takes place near phase singularities. Specifically, we showed that remarkable spectral changes take place in the neighborhood of axial zeros of the intensity near the geometrical focus of a converging, spatially fully coherent, polychromatic spherical wave diffracted at a circular aperture. In particular, we found that the spectrum is redshifted at some points, blueshifted at others, and split into two lines elsewhere.

In the present paper we explore such spectral changes in more detail. In particular, we investigate the strength of the effect. We also show that such spectral changes take place in the neighborhood of phase singularities in the geometrical focal plane (the neighborhood of zeros of the Airy pattern). These predictions have recently been confirmed experimentally by Popescu and Dogariu.[6] It is clear that these recent investigations appreciably broaden the scope of the rapidly developing field of singular optics.

In Section 2 we review those aspects of focusing that are relevant for the understanding of our analysis, describe the changes of the spectrum in the focal region, and discuss the singular behavior of the spectrum on axis. In Section 3 we show that similar anomalous behavior takes place in the neighborhood of the zeros in the geometric focal plane. In Section 4 we describe quantitatively the integrated spectrum (the averaged total intensity) of the field in the focal region and discuss its dependence on the focusing geometry.

2. SPECTRUM IN THE FOCAL REGION

Let us first consider a monochromatic spherical wave of frequency ω, emerging from an aperture of radius a and converging toward an axial focal point O. The focusing configuration is depicted in Fig. 1. We assume that

$$f \gg a \gg \lambda, \tag{1}$$

where f is the radius of the spherical wave in the aperture and $\lambda = 2\pi c/\omega$ is the wavelength of the emergent wave. According to the Huygens–Fresnel principle (Ref. 7, Sec. 8.2), the field at a point $P(\mathbf{r})$ in the region of focus is given by the formula

0740-3232/2002/081694-07$15.00

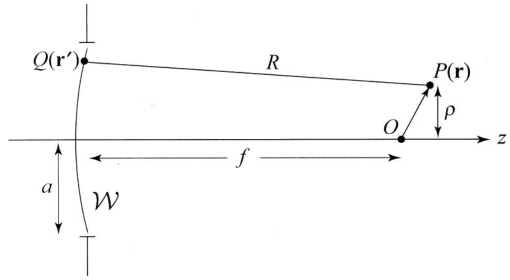

Fig. 1. Notation relating to the focusing geometry. Here $R = |\mathbf{r} - \mathbf{r}'|$.

$$U(\mathbf{r},\ \omega) = -\frac{\mathrm{i}}{\lambda}\int_{\mathcal{W}} U^{(0)}(\mathbf{r}',\ \omega)\frac{\exp(\mathrm{i}k|\mathbf{r} - \mathbf{r}'|)}{|\mathbf{r} - \mathbf{r}'|}\mathrm{d}^2 r', \tag{2}$$

where

$$U^{(0)}(\mathbf{r},\ \omega) = \frac{A(\omega)}{f}\exp(-\mathrm{i}kf) \tag{3}$$

is the field at a point $Q(\mathbf{r}')$ on the wave front $\mathcal{W}$ that momentarily fills the aperture. Here $A(\omega)/f$ is the amplitude, at frequency ω, of the incident field on the wave front $\mathcal{W}$. We assume that the Fresnel number

$$N = \frac{a^2}{\lambda f} \tag{4}$$

of the focusing geometry is much greater than unity. The integral (2) may then be expressed in a form due to Debye (Ref. 7, Sec. 8.8). One then readily finds that

$$U(\mathbf{r},\ \omega) = -2\pi\mathrm{i}N_0\left(\frac{\omega}{\omega_0}\right)\frac{A(\omega)}{f}\exp(\mathrm{i}f^2\omega u_0/a^2\omega_0) \times \int_0^1 J_0(\omega v_0\xi/\omega_0)\exp(-\mathrm{i}\omega u_0\xi^2/2\omega_0)\xi\mathrm{d}\xi, \tag{5}$$

where, for convenience, we have introduced an (as yet) undefined frequency ω_0 to be used as a scaling parameter, and where

$$N_0 = \frac{a^2}{\lambda_0 f} \tag{6}$$

is the Fresnel number at frequency ω_0, $\lambda_0 = 2\pi c/\omega_0$, J_0 is the Bessel function of the first kind and order zero, and the dimensionless spatial variables u_0 and v_0 (sometimes called the Lommel variables) are defined by the expressions

$$u_0 = 2\pi N_0\frac{z}{f}, \tag{7}$$

$$v_0 = 2\pi N_0\frac{\rho}{a}. \tag{8}$$

It is to be noted that u_0, v_0 are scaled differently and that $U(\mathbf{r},\ \omega)$ is independent of the arbitrarily chosen frequency ω_0. Expression (5), together with Eqs. (6), (7), and (8), can be used to determine the field at any point in the three-dimensional region around the geometric focus.

Suppose next that the field is not monochromatic but rather is a polychromatic wave. For such a wave field one must consider, instead of the incident field $U^{(0)}(\mathbf{r},\ \omega)$, the cross spectral density function of the incident field,

$$W^{(0)}(\mathbf{r}',\ \mathbf{r}'',\ \omega) \equiv \langle U^{(0)*}(\mathbf{r}',\ \omega)U^{(0)}(\mathbf{r}'',\ \omega)\rangle, \tag{9}$$

where the angle brackets denote the average, taken over a statistical ensemble of monochromatic realizations $\{U^{(0)}(\mathbf{r}')\exp(-\mathrm{i}\omega t)\}$ (Ref. 8, Sec. 4.7). A similar definition holds for the cross-spectral density $W(\mathbf{r}',\ \mathbf{r}'',\ \omega)$ of the focused field.

It follows from the definition of the cross-spectral density and from Eq. (2) that

$$W(\mathbf{r}_1,\ \mathbf{r}_2,\ \omega) = \frac{1}{\lambda^2}\int\int_{\mathcal{W}} W^{(0)}(\mathbf{r}_1',\ \mathbf{r}_2',\ \omega) \times \frac{\exp(-\mathrm{i}k|\mathbf{r}_1 - \mathbf{r}_1'|)}{|\mathbf{r}_1 - \mathbf{r}_1'|}\frac{\exp(\mathrm{i}k|\mathbf{r}_2 - \mathbf{r}_2'|)}{|\mathbf{r}_2 - \mathbf{r}_2'|} \times \mathrm{d}^2 r_1'\mathrm{d}^2 r_2'. \tag{10}$$

Evidently the spectrum of the field at a point $P(\mathbf{r})$ in the focal region is given by

$$S(\mathbf{r},\ \omega) \equiv W(\mathbf{r},\ \mathbf{r},\ \omega) = \frac{1}{\lambda^2}\int\int_{\mathcal{W}} W^{(0)}(\mathbf{r}_1',\ \mathbf{r}_2',\ \omega) \times \frac{\exp(-\mathrm{i}k|\mathbf{r} - \mathbf{r}_1'|)}{|\mathbf{r} - \mathbf{r}_1'|}\frac{\exp(\mathrm{i}k|\mathbf{r} - \mathbf{r}_2'|)}{|\mathbf{r} - \mathbf{r}_2'|}\mathrm{d}^2 r_1'\mathrm{d}^2 r_2'. \tag{11}$$

We will take the incident field in the aperture to be a spatially fully coherent, polychromatic spherical wave of constant amplitude. The cross-spectral density at points $Q(\mathbf{r}_1')$ and $Q(\mathbf{r}_2')$ on the wave front $\mathcal{W}$ is then given by the expression

$$W^{(0)}(\mathbf{r}_1',\ \mathbf{r}_2',\ \omega) = \frac{|A(\omega)|^2}{f^2}. \tag{12}$$

On substituting from Eq. (12) into Eq. (11), and using formula (5), we readily find that

$$S(\mathbf{r},\ \omega) = M(\mathbf{r},\ \omega)S^{(0)}(\omega), \tag{13}$$

where

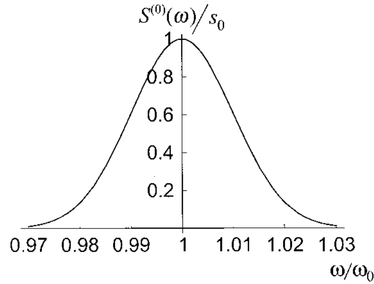

Fig. 2. Plot of the spectrum of the incident field for $\sigma_0/\omega_0 = 0.01$.

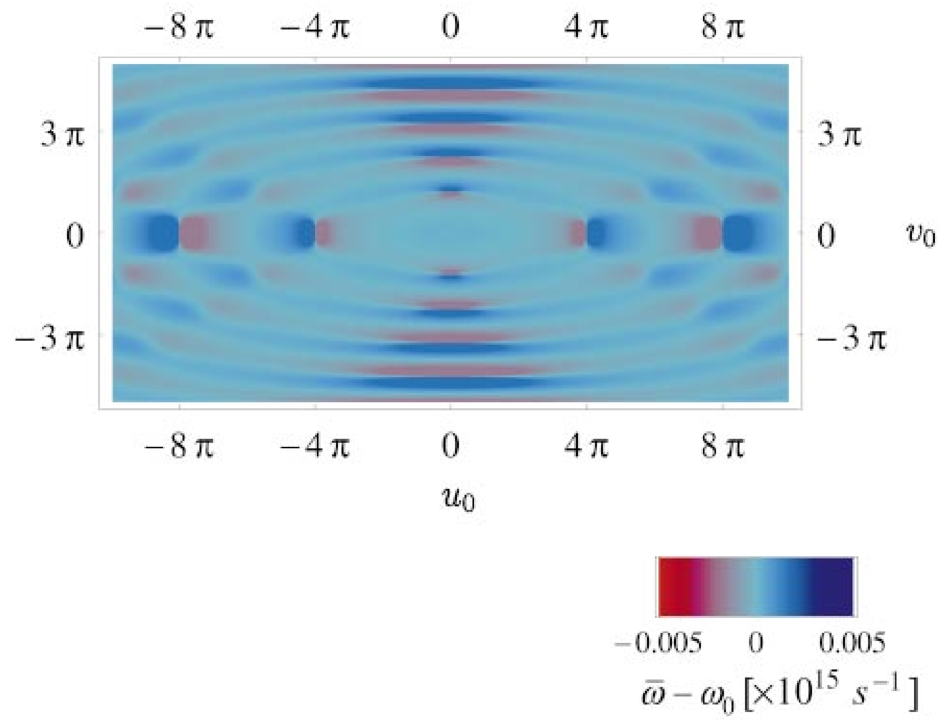

Fig. 3. Color-coded plot of the mean frequency $\bar{\omega}$ of the spectrum in the focal region as a function of u_0, v_0, for $\omega_0 = 10^{15}\ \mathrm{s}^{-1}$, $\sigma_0 = 10^{13}\ \mathrm{s}^{-1}$, and $N_0 = 100$. The color is more red or blue as the spectrum is more redshifted or blueshifted, respectively.

$$S^{(0)}(\omega) \equiv \frac{|A(\omega)|^2}{f^2} \tag{14}$$

is the spectrum of the incident field in the aperture, and

$$M(\mathbf{r},\ \omega) \equiv (2\pi N_0)^2 \left(\frac{\omega}{\omega_0}\right)^2 \left| \int_0^1 J_0(\omega v_0 \xi/\omega_0) \times \exp[-\mathrm{i}\omega u_0 \xi^2/2\omega_0]\xi \mathrm{d}\xi \right|^2. \tag{15}$$

It can be seen from Eq. (13) that the spectrum of the field in the focal region is given by the spectrum of the incident wave multiplied by the function $M(\mathbf{r},\ \omega)$, sometimes called the *spectral modifier*.

Equations (13), (14), and (15) can be used to determine the spectrum at any point in the focal region. Because the spectral modifier depends on both position and frequency, it is clear that the spectrum will, in general, be different at different points and will differ from the spectrum of the incident field. To illustrate such changes, we assume the spectrum of the incident field to consist of a single line of Gaussian form (see Fig. 2); i.e.,

$$S^{(0)}(\omega) = s_0 \exp[-(\omega - \omega_0)^2/2\sigma_0^2]. \tag{16}$$

Here s_0 is a positive constant, σ_0 is the bandwidth, and ω_0 is the center frequency. We assume that the field is quasi-monochromatic ($\sigma_0/\omega_0 \ll 1$). We choose the arbitrary frequency ω_0 introduced in Eq. (5) to be equal to the center frequency; therefore the normalized coordinates u_0, v_0 are defined with respect to the dominant frequency in the incident spectrum. It should be noted, though, that this choice is a matter of convenience. If the spectrum of the incident field has a more complicated shape (multiple lines, asymmetric lines, etc.), other choices may be more appropriate.

The spectrum in the focal region can be characterized by its various moments, such as the mean frequency, $\bar{\omega}(\mathbf{r})$, defined as

$$\bar{\omega}(\mathbf{r}) = \frac{\int \omega' S(\mathbf{r},\ \omega')\mathrm{d}\omega'}{\int S(\mathbf{r},\ \omega')\mathrm{d}\omega'}. \tag{17}$$

The mean frequency is plotted as a function of u_0, v_0 in Fig. 3, for $\omega_0 = 10^{15}\ \mathrm{s}^{-1}$, $\sigma_0 = 10^{13}\ \mathrm{s}^{-1}$, and $N_0 = 100$. The color is more red or more blue as the spectrum is more redshifted or blueshifted, respectively. It can be seen from the figure that, although there are some changes of the spectrum throughout the focal region, the most drastic changes occur at points on the u_0 axis where u_0 is a multiple of 4π and on the v_0 axis (geometric focal plane) where v_0 is a zero of the Bessel function of the first kind and order one. These drastic changes arise from zeros in the modifier function $M(\mathbf{r},\ \omega)$; we briefly review the behavior of the spectrum on the u_0 axis, which was discussed in some detail in our earlier paper.[5] In Section 3 we discuss the behavior on the v_0 axis.

On the u_0 axis, the modifier function can readily be shown to have the simple form (Ref. 7, Sec. 8.8)

$$M(u_0,\ 0,\ \omega) = (\pi N_0)^2 \left(\frac{\omega}{\omega_0}\right)^2 \left[\frac{\sin(\omega u_0/4\omega_0)}{\omega u_0/4\omega_0}\right]^2. \tag{18}$$

It can be seen from Eq. (18) that at points where $u_0 = 4\pi n$ and n is a nonzero integer, the modifier function is zero at frequency ω_0. Modifications in the spectrum as the point of observation is changed arise from the change in the position of this zero with respect to frequency. In Fig. 4 the spectrum is shown at $u_0 = 4\pi$ and at two points immediately to the left and right of it, at distance $\delta = 0.15$. It can be seen that at $u_0 = 4\pi$ the spectrum is split into two peaks: at $u_0 = 4\pi - \delta$ it is redshifted, and at $u_0 = 4\pi + \delta$ it is blueshifted.

These points on the u_0 axis, where the modifer function is zero at the center frequency, are truly singular points of the spectral distribution, as we now show. We consider the standard deviation of the spectrum from the mean frequency, viz.,

$$\Delta\omega(\mathbf{r}) = \left[\frac{\int [\omega' - \bar{\omega}(\mathbf{r})]^2 S(\mathbf{r}, \omega') \mathrm{d}\omega'}{\int S(\mathbf{r}, \omega') \mathrm{d}\omega'} \right]^{1/2}. \quad (19)$$

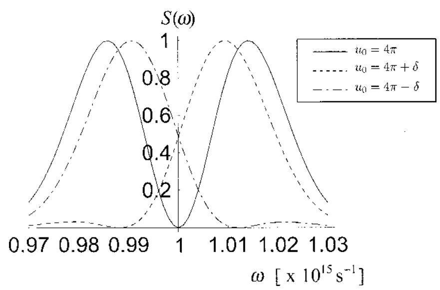

Fig. 4. Depiction of the spectral changes on and about the axial zero $u_0 = 4\pi$, for $\omega_0 = 10^{15}\ \mathrm{s}^{-1}$, $\sigma_0 = 10^{13}\ \mathrm{s}^{-1}$, and $N_0 = 100$, with $\delta = 0.15$. The peak values of each of the spectra are normalized to unity.

It is to be noted that the modifier function $M(\mathbf{r}, \omega)$ is a smooth function of frequency for all values of u_0 and v_0. We may therefore expand it in a Taylor series about the center frequency ω_0. For an incident field of sufficiently narrow bandwidth σ_0, the modifier function may be represented by the lowest-order term of its Taylor series for all frequencies of the spectrum of the incident field. For instance, for those positions $(u_0, 0)$ such that the modifier function has no zeros within σ_0 of the center frequency ω_0, we may approximate $M(\mathbf{r}, \omega)$ by a constant,

$$M(u_0, 0, \omega) \approx M(u_0, 0, \omega_0). \quad (20)$$

For such nonsingular positions, the spectrum in the focal region is therefore proportional to the spectrum of the incident field. On substitution from Eqs. (20) and (16) into Eq. (19) it can be seen that

$$\Delta\omega(u_0, 0) = \sigma_0 \qquad \text{(nonsingular position)}. \quad (21)$$

In contrast, at the singular points $(u_0 = 4\pi n)$, the leading-order term in the Taylor expansion of $M(\mathbf{r}, \omega)$ is quadratic, namely,

$$M(4\pi n, 0, \omega) \approx \frac{(\pi N_0)^2}{2} \frac{\partial^2}{\partial\omega^2} \left[\frac{\sin(\omega n \pi/\omega_0)}{n\pi} \right]^2_{\omega=\omega_0} (\omega - \omega_0)^2 = \left(\frac{\pi N_0}{\omega_0} \right)^2 (\omega - \omega_0)^2. \quad (22)$$

The local behavior of the modifier function at the singular points is given by relation (22), whereas for the nonsingular points it is given by relation (20). The local behavior of the modifier function is therefore fundamentally differ-

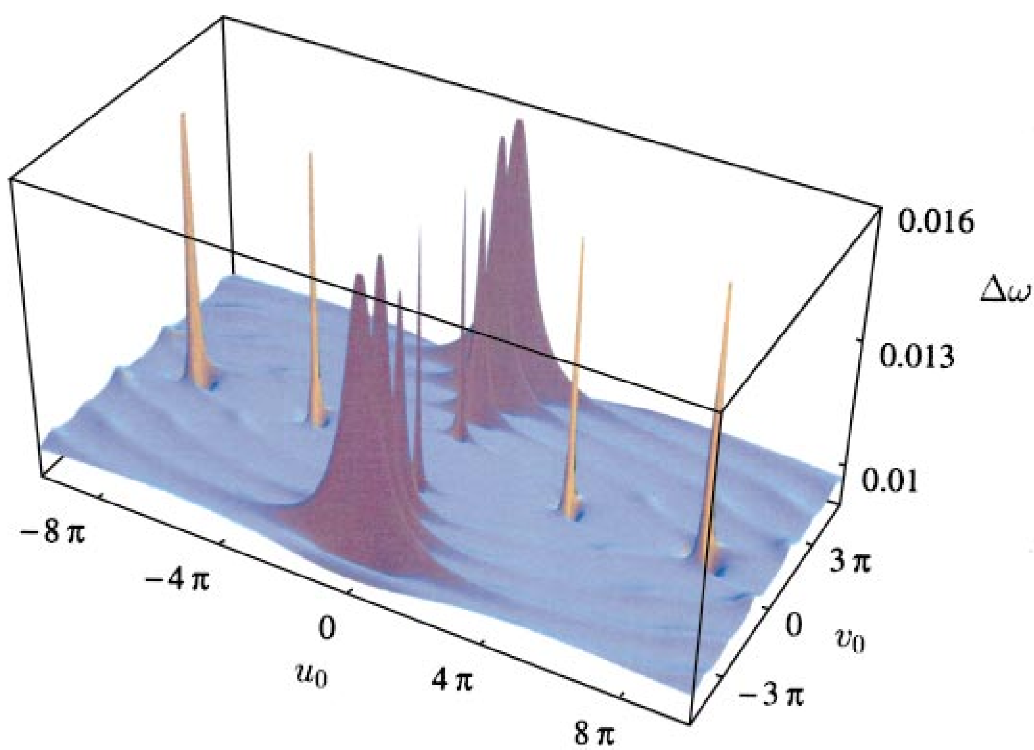

Fig. 5. The standard deviation $\Delta\omega$ of the spectrum about the frequency ω_0, as a function of position u_0, v_0, with $\omega_0 = 10^{15}\ \mathrm{s}^{-1}$, $\sigma_0 = 10^{13}\ \mathrm{s}^{-1}$, and $N_0 = 100$.

ent at the singular points. It can be shown on substitution from Eq. (22) into Eq. (19) that

$$\Delta\omega(u_0, 0) = \sqrt{3}\sigma_0 \qquad \text{(singular position)}. \tag{23}$$

The standard deviation is therefore greater at a singular point than at an ordinary point. We note that Eqs. (21) and (23) hold for any sufficiently small values of σ_0; at the singular points, the standard deviation of the spectrum will always be greater than the standard deviation of the spectrum of the incident field.

The standard deviation is displayed in three-dimensional form in Fig. 5, for $\omega_0 = 10^{15}\ \text{s}^{-1}$, $\sigma_0 = 10^{13}\ \text{s}^{-1}$, and $N_0 = 100$. As predicted, the standard deviation exhibits narrow peaks at the points where $u_0 = 4\pi n$, n being any nonzero integer.

It should be noted, though, that the spatial location of the singular points arises not only from the geometry of focusing and the center frequency but also from the shape of the incident spectrum. An incident field with a multiline or asymmetric line shape will exhibit behavior different from what we have just discussed, even if the center (mean) frequency of the incident spectrum is the same as that of a single, symmetric line.

3. SINGULAR BEHAVIOR IN THE FOCAL PLANE

In the previous section, we saw how drastic changes of the spectrum on axis in the focal region arise from the zeros of the modifier function. Figure 3 shows that similar drastic changes also occur in the geometric focal plane (v_0 axis) at nearly regular intervals, and it is reasonable to expect that they appear for the same reason.

In the geometric focal plane, it can be shown (Ref. 7, Sec. 8.8) that the spectral modifier function takes on the simple form

$$M(0, v_0, \omega) = (2\pi N_0)^2 \left(\frac{\omega}{\omega_0}\right)^2 \left[\frac{J_1(\omega v_0/\omega_0)}{(\omega v_0/\omega_0)}\right]^2, \tag{24}$$

where J_1 is the Bessel function of the first kind and order one. It can be seen from Eq. (24) that at points for which $J_1(v_0) = 0$ (i.e., at zeros of the Airy pattern at frequency ω_0), the modifier function is zero at that frequency. The first three zeros of the Bessel function J_1 are $v_0 = 3.83, 7.01, 10.17$. The drastic change of the spectrum at such points can be attributed (as were those on the u_0 axis) to the zeros of the modifier function.

We may consider these changes in more detail by examining the spectrum at several points on a small circle of radius δ in the u_0, v_0 plane centered on the point $u_0 = 0$, $v_0 = 3.83$, i.e.,

$$u_0^2 + (v_0 - 3.83)^2 = \delta^2. \tag{25}$$

The spectrum at various points around the circle is illustrated schematically in Fig. 6. It can be seen, as before, that the spectral changes are due to the suppression of some of the components of the spectrum of the incident field.

There is an appreciable topological difference between the singular points on the u_0 axis ($v_0 = 0$) and those in the geometric focal plane ($u_0 = 0$). The spectral singularities on axis are isolated points. However, owing to the rotational symmetry of the modifier function about the u_0 axis, the spectral singularities in the focal plane consist of closed curves. In Fig. 7 the mean frequency of the spectrum [defined in Eq. (17)] in the focal plane u_0

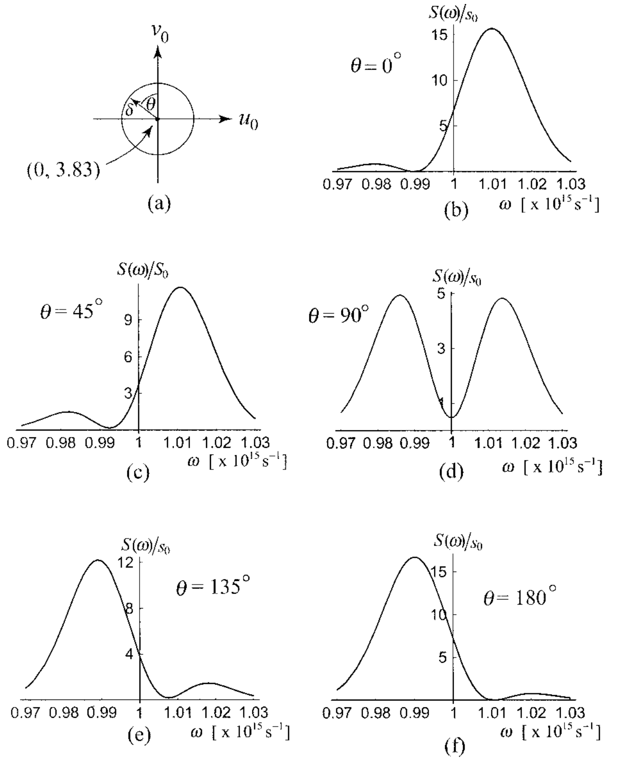

Fig. 6. The spectrum at various points around the first zero in the geometrical focal plane at $u_0 = 0$, $v_0 = 3.83$. (a) The geometry, (b)–(f) the changes in the spectrum at various positions around the circle in the u_0, v_0 plane of radius $\delta = 0.04$.

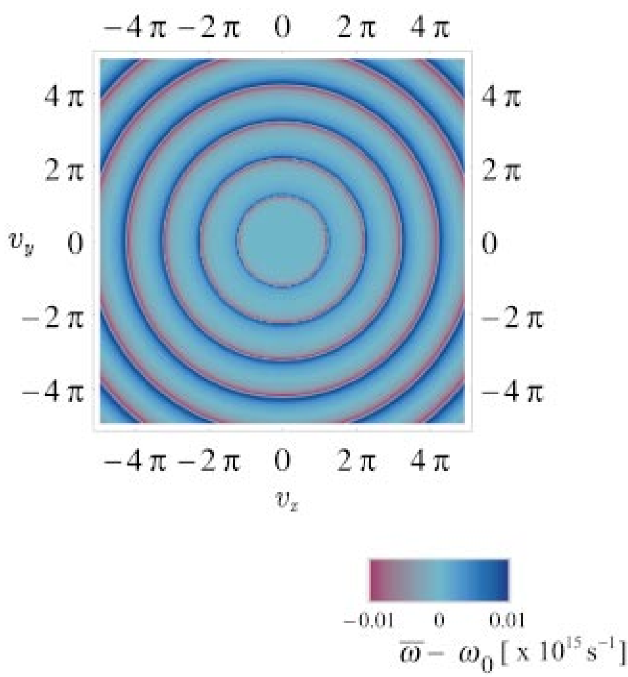

Fig. 7. Color-coded plot of the mean frequency $\bar{\omega}$ of the spectrum in the geometrical focal plane, $u_0 = 0$, for $\omega_0 = 10^{15}\ \text{s}^{-1}$, $\sigma_0 = 10^{13}\ \text{s}^{-1}$, and $N_0 = 100$.

$= 0$ is plotted as a function of transverse coordinates v_x, v_y. It is seen that the spectrum changes drastically as one crosses the circles of $(v_x^2 + v_y^2)^{1/2} = 3.83, 7.01, 10.17$ radii. On these circles, the standard deviation of the spectrum will be greater than that of the spectrum of the incident field. This can be shown in a manner identical to that used in deriving Eq. (23), by using the lowest-order term of the Taylor expansion of the modifier function at the singular points. One then finds that the variance takes on the value given by Eq. (23) at the singular points, as can be seen in Fig. 5.

It should be mentioned that the phase structure around circles of zero intensity has recently been discussed for interfering monochromatic Gaussian beams.[9]

4. INTENSITY IN THE NEIGHBORHOOD OF SPECTRAL SINGULARITIES

So far we have discussed only the changes of the shape of the spectrum relative to the shape of the spectrum of the incident field. We have seen, though, that these changes arise mainly because certain frequencies of the incident spectrum are suppressed by diffraction, and the total intensity of the field at the singular points is therefore expected to be greatly reduced. In this section we give estimates of the magnitude of this reduction. We also discuss the distances over which the spectrum changes drastically.

We first consider the spectrum of the field at the axial singularities, $u_0 = 4\pi n$, $v_0 = 0$. We assume again that the spectrum of the incident field is a narrow-band Gaussian distribution ($\sigma_0 \ll \omega_0$), and hence we may again approximate the modifier function by relation (22). The spectrum at the axial singularities is then given by

$$S(4\pi n, 0, \omega) \approx \left(\frac{\pi N_0}{\omega_0}\right)^2 (\omega - \omega_0)^2 s_0 \times \exp[-(\omega - \omega_0)^2/2\sigma_0^2]. \quad (26)$$

The total intensity[10] at a point (u_0, v_0) is defined by the expression

$$I(u_0, v_0) \equiv \int_0^\infty S(u_0, v_0, \omega')\mathrm{d}\omega'. \quad (27)$$

At the axial singular points, it is then found to be

$$I(4\pi n, 0) = \frac{1}{2}(2\sigma_0^2)^{3/2}\sqrt{\pi}s_0\left(\frac{\pi N_0}{\omega_0}\right)^2. \quad (28)$$

We note that the intensity at the geometric focus ($u_0 = v_0 = 0$) is given by the expression

$$I(0, 0) = \sqrt{2\pi\sigma_0^2}(\pi N_0)^2 s_0, \quad (29)$$

and hence the normalized intensity at the axial singular points is given by

$$\frac{I(4\pi n, 0)}{I(0, 0)} = \left(\frac{\sigma_0}{\omega_0}\right)^2. \quad (30)$$

We see that, with an incident field of sufficiently narrow bandwidth, the intensity at the axial singular points is reduced from that at the geometric focus by the square of the fractional bandwidth, σ_0/ω_0. If, for instance, the fractional bandwidth is 1%, the intensity at the singular points on axis will be smaller by a factor of 10^4 than the intensity at the geometric focus. The behavior of the intensity on axis, calculated from Eqs. (13) and (15), is shown in Fig. 8. The inset shows an extended view about the first two singular points on axis. The value of the intensity at these two points is in good agreement with that given by Eq. (30).

We may also determine the intensity at the singularities in the focal plane. For narrow-band light, the modifier function has the approximate form

$$M(0, v_n, \omega) \approx \frac{(2\pi N_0)^2}{\omega_0^2}(J_2[v_n])^2(\omega - \omega_0)^2, \quad (31)$$

where v_n is the nth zero of the Bessel function $J_1(v)$. In a manner identical to that used to derive Eq. (30), we find that

$$\frac{I(0, v_n)}{I(0, 0)} = \frac{4\sigma_0^2}{\omega_0^2}(J_2[v_n])^2. \quad (32)$$

The behavior of the intensity in the focal plane is shown in Fig. 9.

Up to this point we have used only the dimensionless coordinates u_0, v_0. Another question of practical interest concerns the physical size of the region over which the spectrum changes drastically, and we now address this problem. It is reasonable to assume that the maximum red or blue shifts will occur when the modifier function, and therefore the spectrum in the focal region, has a zero at frequency $\omega_0 + \sigma_0$ or $\omega_0 - \sigma_0$, respectively. We consider the first singular point on the z axis. The modifier function will have a zero at the center frequency at $u_{4\pi} = 4\pi$, and it will have a zero at frequencies $\omega_0 \pm \sigma_0$ at the points $u_\pm = 4\pi\omega_0/(\omega_0 \pm \sigma_0)$. The distance Δu between the singular point $u_{4\pi}$ and the points of maximum shift $u_\pm$ is

$$\Delta u \equiv u_{4\pi} - u_\pm \approx \pm\frac{4\pi\sigma_0}{\omega_0}. \quad (33)$$

In deriving Eq. (33) we have used the fact that $\sigma_0 \ll \omega_0$. For $\sigma_0/\omega_0 = 0.01$, one has $\Delta u = 0.12$. We may use Eq.

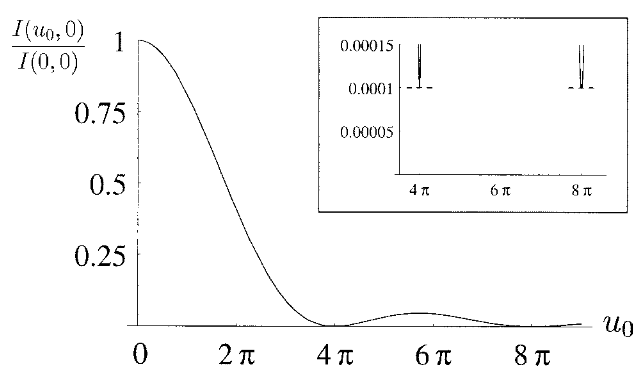

Fig. 8. Total intensity $I(u_0, 0)$ on axis in the focal region, with $\omega_0 = 10^{15}\ \mathrm{s}^{-1}$, $\sigma_0 = 10^{13}\ \mathrm{s}^{-1}$, and $N_0 = 100$. The inset shows an expanded view about the first two singular points. The dashed lines indicate the values predicted by Eq. (30).

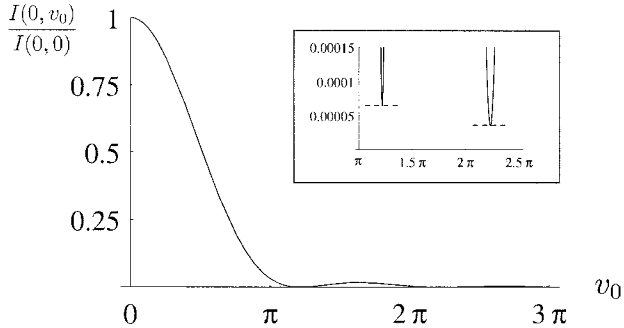

Fig. 9. The total intensity $I(0, v_0)$ in the focal plane, with $\omega_0 = 10^{15}\ \mathrm{s}^{-1}$, $\sigma_0 = 10^{13}\ \mathrm{s}^{-1}$, and $N_0 = 100$. The inset shows an expanded view about the first two singular points. The dashed lines indicate the values predicted by Eq. (32).

(7) to express $u_{4\pi}$, $u_\pm$ in terms of physical distances $z_{4\pi}$, $z_\pm$. It can readily be shown that

$$\frac{\Delta z}{\lambda_0} = \frac{z_{4\pi} - z_\pm}{\lambda_0} \approx \pm 2\left(\frac{f}{a}\right)^2 \frac{\sigma_0}{\omega_0}. \tag{34}$$

If, for example, $f/a = 10$ and $\sigma_0/\omega_0 = 0.01$, Δz is of the order of a wavelength.

We may perform a similar calculation with regard to the first singularity in the focal plane. At the center frequency ω_0, the spectrum has a zero at $v_1 = 3.83$, and it will have zeros at frequencies $\omega_0 \pm \sigma_0$ for $v_\pm = 3.83\omega_0/(\omega_0 \pm \sigma_0)$. The maximum spectral shifts will therefore occur at v distances such that

$$\Delta v \equiv v_1 - v_\pm \approx \pm \frac{3.83\sigma_0}{\omega_0}. \tag{35}$$

For $\sigma_0/\omega_0 = 0.01$, one has $\Delta v = 0.04$. In terms of the actual distance $\Delta\rho$ in the focal plane, it can readily be shown that

$$\frac{\Delta\rho}{\lambda_0} = \pm \frac{3.83}{2\pi}\left(\frac{f}{a}\right)\left(\frac{\sigma_0}{\omega_0}\right). \tag{36}$$

It is to be noted that this distance, with $f/a = 10$, is smaller by an order of magnitude than the distance Δz on axis. Detecting the spectral changes in the focal plane will therefore require greater spatial resolution than detection of those on the u_0 axis.

ACKNOWLEDGMENTS

This research was supported by the U.S. Air Force Office of Scientific Research under grant F49260-96-1-400, by the Engineering Research Program of the Office of Basic Energy Science at the U.S. Department of Energy under grant DE-FG02-90-ER 14119, by the Dutch Technology Foundation (STW), and by the European Union within the framework of the Future and Emerging Technologies–SLAM program.

Corresponding author E. Wolf can be reached at the address on the title page or by e-mail, ewlupus @pas.rochester.edu.

REFERENCES AND NOTES

1. A pioneering paper on this subject is due to J. F. Nye and M. V. Berry, “Dislocation in wavetrains,” Proc. R. Soc. London Ser. A **336**, 165–190 (1974).
2. For a review of singular optics see, for example, M. S. Soskin and M. V. Vasnetsov, “Singular optics,” in *Progress in Optics*, E. Wolf, ed. (Elsevier, Amsterdam, 2001), Vol. 42, pp. 219–276.
3. M. V. Berry and A. N. Wilson, “Black-and-white fringes and the colors of caustics,” Appl. Opt. **33**, 4714–4718 (1994).
4. M. V. Berry and S. Klein, “Colored diffraction catastrophes,” Proc. Natl. Acad. Sci. U.S.A. **93**, 2614–2619 (1996).
5. G. Gbur, T. D. Visser, and E. Wolf, “Anomalous behavior of spectra near phase singularities of focused waves,” Phys. Rev. Lett. **88**, 013901 (2002).
6. G. Popescu and A. Dogariu, “Spectral anomalies at wavefront dislocations,” Phys. Rev. Lett. **88**, 183902 (2002).
7. M. Born and E. Wolf, *Principles of Optics*, 7th (expanded) ed. (Cambridge U. Press, Cambridge, UK, 1999).
8. L. Mandel and E. Wolf, *Optical Coherence and Quantum Optics* (Cambridge U. Press, Cambridge, UK, 1995).
9. V. A. Pas’ko, M. S. Soskin, and M. V. Vasnetsov, “Transversal optical vortex,” Opt. Commun. **198**, 49–56 (2001).
10. The term “intensity” is used in optics with several different meanings. In this paper we mean by it the frequency-integrated spectrum, as indicated in Eq. (27).